International Journal of Modern Physics B Vol. 3, No. 8 (1989) 1183–1203

SYMBOLIC DYNAMICS ANALYSIS OF SYMMETRY BREAKING AND RESTORATION†

ZHENG WEI-MOU
Center for Theoretical Physics, CCAST (World Laboratory), Institute of Theoretical Physics, Academia Sinica, China

and

HAO BAI-LIN
Institute of Theoretical Physics, Academia Sinica, P. O. Box 2735, Beijing 100080, China

Received 10 March 1989

A bifurcation theory and symbolic dynamics analysis of symmetry breakings and restorations in antisymmetric mappings is carried out. The fact that symmetry breakings are precursors to period-doubling happens to be a natural consequence of word ordering in symbolic dynamics. Symbolic dynamics also provides the selection rule for such bifurcations to occur and helps to locate the symmetry restoration point in the chaotic region. When the inverse branches are known explicitly the analysis may be made detailed enough to determine the bifurcation structure with high precision.

1. Introduction

Symmetry breaking and symmetry restoration are common phenomena in physical systems with a certain kind of symmetry. An equation or a thermodynamical potential may possess a higher symmetry, but a particular solution or an equilibrium state may exhibit only a lower symmetry. However, all these asymmetric solutions (or states) taken together restore the original symmetry. In many physical systems, there exists a mechanism that connects various asymmetric solutions and "helps" to restore the full symmetry, e.g., spin waves in a ferromagnet or Goldstone modes in a field theory with degenerated ground state. In fact, the notion of symmetry breaking has been playing an increasingly important role in understanding diverse problems ranging from continuous phase transitions to the origin of the Universe.

Keywords: chaos, symbolic dynamics, symmetry breaking.

† This Work was partially supported by the Chinese Natural Science Foundation.

PACS Nos.: 05.40+, 05.45+b.

It is interesting to note that a simple form of symmetry breaking and restoration appears in the bifurcation structure of many dynamical systems. It shows clearly in the bifurcation diagram of the antisymmetric cubic map[1-3]:

$$x_{n+1} \equiv f(A, x_n) = Ax_n^3 + (1-A)x_n. \tag{1}$$

(For the graph of (1) see Fig. 1, for the bifurcation diagram see Fig. 2.) The existence of symmetric orbits, which first undergo symmetry-breaking bifurcation into asymmetric orbits, and then enjoy period-doubling, has been observed in numerical studies of many systems of ordinary[4-13] and partial[14] differential equations as well as in laboratory experiments.[15,16] It seems that for the time being the Lorenz model[17,9] is in this respect the most studied system. Since it is invariant under the transformation $x \to -x, y \to -y$, it has been associated with symbolic dynamics of three letters and many cases of symmetry breaking have been described explicitly in terms of symbolic sequences.[13]

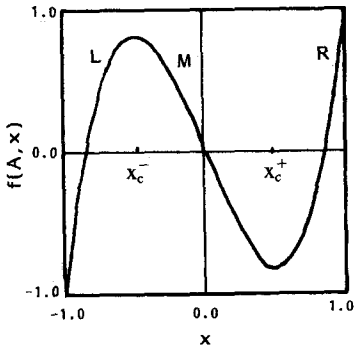

Fig. 1. The antisymmetric cubic map.

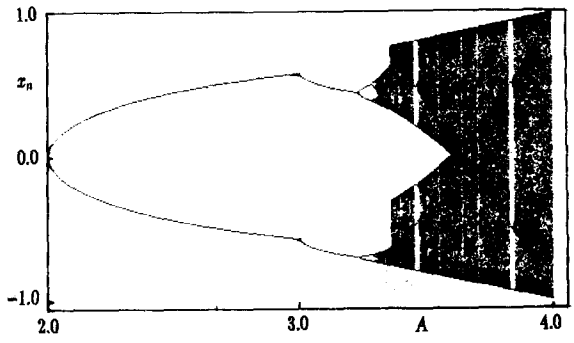

Fig. 2. Bifurcation diagram of the antisymmetric cubic map.

Observations have led to the conjecture that symmetry breaking must precede period-doubling, whence follows the expression "precursor"[15,12] to period-doubling or "suppression"[18,11] of period-doubling by symmetry breaking, etc. The phenomenon was correctly related to the symmetry of the governing equations,[15] and a heuristic explanation based on bifurcation theory was given in Ref. 11. The most complete bifurcation theory analysis applied to the Poincaré mapping of flows appeared in Ref. 18 with the conclusion that a symmetric orbit cannot undergo period-doubling directly except in extraordinary cases.

In contrast to symmetry breakings, the phenomenon of symmetry restoration has rarely been discussed in the literature. There has been, for example, one occasion of mentioning "a bifurcation back to symmetry",[6] but nothing was said about the nature of the bifurcation. Apparently it was addressed to the reverse period-doubling cascade due to non-monotonic parameter dependence, not to the genuine symmetry restoration which, as shown in this paper, must take place in the chaotic region. The mechanism that helps to restore the symmetry is the collision of the unstable symmetric orbit with the chaotic attractor, i.e., a "crisis".

In this paper, we present a detailed symbolic dynamics analysis for symmetry breaking as well as for symmetry restoration. In particular, we are going to show:

1. The bifurcation analysis of symmetry breakings can be carried out simply and thoroughly for general antisymmetric mappings in much the same way as for the tangent or period-doubling bifurcations.[21]
2. Symbolic dynamics determines the precedence of symmetric orbit over the asymmetric ones. It provides a selection rule to pick up those orbits of even periods that are destined to symmetry breaking.
3. Symbolic dynamics furnishes a precise description for symmetry restoration, determining the location of the asymmetry-symmetry transition and indicating the infinite sequence of symmetric orbits that converges backwards to the transition point. The convergence rate is shown to be non-universal.
4. When the inverse branches of the map are known explicitly, the analysis may be accomplished in a down-to-numbers way by invoking the technique of "lifting" words in the symbolic dynamics to equations for parameters.[19,20]
5. Being formulated in the language of symbolic dynamics, the essence of our analysis applies to differential equations as well. Many previous observations may be better understood now. We shall make a few remarks in this respect.

The points listed above also give an idea on the layout of this paper. To have a feeling on antisymmetric maps we start with the cubic map (1).

2. The Antisymmetric Cubic Map

An explicit analysis[1] of the first bifurcations in the antisymmetric cubic map may help us to understand the general case. The map (1) becomes non-monotonic

for $A>1$ when there are two critical points

$$C=\sqrt{(A-1)/3A}, \qquad \bar{C}=-C. \tag{2}$$

(See Fig. 1). It maps the interval $(-1, +1)$ onto itself as long as $0 \le A \le 4$, but for $A \in (0, 1]$ the entire map is monotonic. Therefore, we are interested in the parameter range $(1, 4]$. Among the three fixed points 0 and ± 1, the latter two are always unstable while $x^*=0$ is stable for $0<A<2$, so we follow the stable fixed point $x^*=0$ up to $A=2$, where an ordinary period-doubling takes place, giving rise to a symmetric 2-cycle. To determine its stability range, we note that this 2-cycle is formed by a pair $(x^*, -x^*)$, related by an inversion. The derivative of an odd function is even, so for this symmetric 2-cycle, the stability discriminant

$$s=\left.\frac{\partial f^{(2)}}{\partial x}\right|_{\pm^*}=\left.\frac{\partial f}{\partial x}\right|_{\mp^*}\left.\frac{\partial f}{\partial x}\right|_{\pm^*}=\left(\left.\frac{\partial f}{\partial x}\right|_{*}\right)^2 \ge 0. \tag{3}$$

(We write $|_*$ instead of $|_{x^*}$ hereinafter.) Contrary to an orbit arising from period-doubling s can never get negative: $s=1$ at $A=2$ as it should be when arise from period-doubling, $s=0$ corresponds to a symmetric superstable 2-cycle, and again $s=1$ when it loses stability at $A=3$. It is at the last point where a symmetry-breaking bifurcation occurs.

When A gets larger than 3, the symmetric 2-cycle loses stability. To calculate explicitly the asymmetric 2-cycle, we exclude the trivial zeros of $f^{(2)}-x$, dividing it by the fixed point relation $f-x$ and inversion point relation $(f+x)/x$, i.e.,

$$\frac{f^{(2)}(x)-x}{(f(x)-x)(f(x)+x)/x}=A(A^2x^4+A(1-A)x^2+1). \tag{4}$$

Its two zeros

$$x_{\pm}^*=\sqrt{\frac{A-1\pm\sqrt{(A-3)(A+1)}}{2A}} \tag{5}$$

give rise to two 2-cycles

$$x_+^* \to -x_-^* \to x_+^* \text{ and } x_-^* \to -x_+^* \to x_-^*.$$

They enjoy stability in the same A range

$$3<A<1+\sqrt{5},$$

each in its own basin. Therefore, only one of them may be observed for a given initial value. The stability discriminant s reaches -1 at $A = 1 + \sqrt{5}$ where a period-doubling to a 4-cycle takes place.

In what follows, we shall need the explicit expressions for the inverse branches of the cubic map (1). To solve the equation

$$y = Ax^3 - (A-1)x \tag{6}$$

we rescale the variables, letting

$$x = 2\sqrt{(A-1)/3A}\tilde{x} = 2C\tilde{x}, \quad y = 2C\tilde{y}.$$

Equation (6) can then be expressed through the Chebyshov polynomial

$$\frac{3\tilde{y}}{A-1} = 4\tilde{x}^3 - 3\tilde{x} = T_3(\tilde{x}) = \cos(3\arccos(\tilde{x})).$$

Taking into account the multivalueness of the arccosine function, we get

$$\tilde{x} = \cos\left(\frac{1}{3}\arccos\left(\frac{\tilde{y}}{AC^2}\right) + \frac{2k\pi}{3}\right), \qquad k = 0, \pm 1,$$

We shall always use rescaled x and y, but neglect the tilde for brevity. With this convention in mind and introducing the notation

$$AC^2 = \frac{A-1}{3} \equiv a. \tag{7}$$

We shall name the three inverse functions by their labels R, L, and M shown in Fig. 1 as follows:

$$\begin{aligned} R(a,x) &= \cos\left(\frac{1}{3}\arccos\left(\frac{x}{a}\right)\right), \\ L(a,x) &= \cos\left(\frac{1}{3}\arccos\left(\frac{x}{a}\right) + \frac{2\pi}{3}\right), \\ M(a,x) &= \cos\left(\frac{1}{3}\arccos\left(\frac{x}{a}\right) - \frac{2\pi}{3}\right). \end{aligned} \tag{8}$$

We note the following symmetry property of these functions

$$R(a,-x) = -L(a,x),$$
$$M(a,-x) = -M(a,x). \tag{9}$$

Consequently, any composite function $W(a,x)$ made of these functions has the property

$$W(a,-x) = -\bar{W}(a,x)$$

where $\bar{W}$ is obtained from W by interchanging R and L but leaving M unchanged. Sometimes we say that $\bar{W}$ is the mirror image of W. Therefore, dragging a minus sign through a composite function is equivalent to taking its mirror image.

3. The General Case of Symmetry-Breaking Bifurcation

From now on we will consider a general map

$$x_{n+1} = F(A, x_n), \tag{10}$$

where the function F is antisymmetric and depends on a parameter A:

$$F(A,-x) = -F(A,x), \qquad \forall\, x. \tag{11}$$

Note that the k-th iterate of F is also antisymmetric:

$$F^{(k)}(A,-x) \equiv \underbrace{F\circ F\circ \ldots \circ F}_{k \text{ times}}(A,-x) = -F^{(k)}(A,x). \tag{12}$$

Moreover, all odd order derivatives of F with respect to x are even functions, while even order derivatives are odd functions of x.

Suppose that the iteration reaches an *inversion point* x^*

$$x^* = -F(A,x^*), \tag{13}$$

then x^* must be a fixed point of $F^{(2)}$, i.e., a symmetric 2-cycle

$$x^*, -x^*, x^*, -x^*, x^*, \ldots .$$

One can check the stability of the inversion point as well as the stability of the 2-cycle. When the inversion point is no longer stable, a symmetry-breaking bifurcation takes place and gives rise to a pair of asymmetric 2-cycles:

$$x_1^*, -x_2^*, x_1^*, -x_2^*, \ldots ,$$

($|x_1^*| \neq |x_2^*|$) and its mirror image

$$-x_1^*, x_2^*, -x_1^*, x_2^*, \ldots .$$

We are interested in the formulation of the conditions when this happens.

In general, when there is an inversion point for a certain iterate

$$x^* = -F^{(k)}(A, x^*), \tag{14}$$

it must be a $2k$-cycle of F, i.e., a fixed point of $F^{(2k)}$

$$\pm x^* = F^{(2k)}(A, \pm x^*). \tag{15}$$

Therefore, double application of the inversion relation leads to an even period. However, not all even periods may be decomposed into two consecutive inversions. The appropriate criterion will be given later in Sec. 4, using symbolic dynamics. For the time being, we will ask the question: under what conditions can an inversion point lose stability and cause symmetry-breaking bifurcation to occur.

The analysis furnishes a simple and clear example of applying the implicit function theorem in the bifurcation theory and proceeds much like that for period-doubling bifurcation, given by, e.g., Guckenheimer.[21] The difference of these two cases consists of the fact that while many partial derivatives encountered in the analysis of Guckenheimer vanish due to the period-doubling condition

$$\left.\frac{\partial F}{\partial x}\right|_{x^*} = -1,$$

they now disappear as a result of the antisymmetry conditions. To our best knowledge, such a detailed analysis has not yet appeared in the literature. Being carried back to the period-doubling case, our presentation provides also a few technical improvements. For this reason, we will describe it in some detail in the Appendix. We formulate here only the conditions and the

Proposition. Suppose $F(A,x)$: $I-I$ is an antisymmetric map of the interval I onto itself and the following conditions hold:

1. There is an inversion point x^* at the parameter value A^*

$$x^* = -F(A^*, x^*).$$

   It is then a fixed point of $F^{(2)}$.

2. The stability is marginal with the only possibility that

$$\left.\frac{\partial F}{\partial x}\right|_{x^*} = \left.\frac{\partial F}{\partial x}\right|_{-x^*} = 1.$$

3. The Schwarzian derivative $S(F,x)|_{x^*} < 0$. This condition holds automatically for most maps of physical interest, because they do have negative Schwarzian derivatives on the whole interval I, not only at the point x^*.
4. The mixed second derivative of the second iterate does not vanish:

$$\left.\frac{\partial^2 F^{(2)}}{\partial x \partial A}\right|_{x^*} \neq 0.$$

Then on one side of A^* (which side depends on the sign of the mixed derivative that figures in Condition 4, there exists a stable symmetric 2-cycle, which undergoes symmetry-breaking bifurcation at $A = A^*$ into a pair of asymmetric 2-cycles, both stable but observable in their own basins.

4. Symbolic Dynamics as Selection Rule for Symmetry Breakings

Symbolic dynamics of the cubic map has been developed elsewhere.[22,23] We briefly sketch what will be needed in the sequel. We label the three monotonic branches of the map of the letters R, M and L, as denoted in Fig. 1. Then any numerical orbit

$$x_0, x_1 = f(x_0), \ldots, x_n = f(x_{n-1}), \ldots,$$

finite or infinite, may be replaced by a "word" made of these letters. The letters C or/and $\bar{C}$ may appear in a word if the corresponding orbit contains one or both of the critical points (2). The monotonic decreasing branch M is assigned an odd parity, whereas R and L — an even parity. C and $\bar{C}$ may be assigned "zero" parity for convenience. The parity of a symbolic sequence is determined by the number of M's it contains.

Referring to the natural order

$$L < \bar{C} < M < C < R \tag{16}$$

an ordering of symbolic sequences is introduced as follows. Given two words $W_1 = W^*\sigma \ldots$ and $W_2 = W^*\tau \ldots$ where W^* denotes their common leading pattern and $\sigma \neq \tau$, then the order of the two words is the order of σ and τ if the parity of W^* is even, otherwise it is the anti-order of σ and τ, i.e.,

$$\begin{aligned} &W_1 > W_2 \text{ if } \sigma > \tau \text{ when } W^* \text{ is even,} \\ &W_1 > W_2 \text{ if } \sigma > \tau \text{ when } W^* \text{ is odd.} \end{aligned} \tag{17}$$

A symbolic sequence Σ is called a *maximal* sequence, if it is larger than or equal to all shifts $\mathcal{S}^k\Sigma$, where $\mathcal{S}$ denotes the left-shift operator, i.e.,

$$\mathcal{S}\sigma_1\sigma_2\sigma_3\ldots = \sigma_2\sigma_3\ldots$$

and

$$\mathcal{S}^k = \underbrace{\mathcal{S}\mathcal{S}\ldots\mathcal{S}}_{k \text{ times}} .$$

In particular, a periodic sequence

$$(\sigma_1\sigma_2\ldots\sigma_n)^\infty$$

represents the same orbit under cyclic shift of n letters. We take the convention of always writing the maximal sequence.

Starting the iteration from $\bar{C}$, one gets a largest (in the sense of the above ordering) sequence or itinerary $I_{\bar{C}}$, it denotes also the point $f(\bar{C})$ on the interval. Starting from C, one gets a smallest itinerary I_C, represented by another point $f(C)$ on the interval. For a mapping function with negative Schwarzian derivative everywhere, any initial value that is larger than $I_{\bar{C}}$ or smaller than I_C will eventually enter the interval $(I_C, I_{\bar{C}})$, leaving apart a transient. Therefore, we can confine ourselves to this interval only. In general, sequences satisfy the *compatibility condition*

$$I_C < \mathcal{S}^k\Sigma < I_{\bar{C}}. \tag{18}$$

For antisymmetric maps I_C is the mirror image of $I_{\bar{C}}$.

A superstable orbit must contain the letter C or $\bar{C}$, or both. An *asymmetric* superstable orbit contains only one of the critical point, while a *symmetric* one must be of the form

$$\Sigma C\bar{\Sigma}\bar{C} \tag{19}$$

where $\bar{\Sigma}$ is the mirror image of Σ.

An asymmetric superstable orbit $\Sigma\bar{C}$ can be extended to a "window" according to the periodic window theorem[23-25] by changing the last $\bar{C}$ into M and L and arranging the three words in ascending order:

$$\begin{aligned} &\text{If } \Sigma \text{ is even: } (\Sigma L, \Sigma\bar{C}, \Sigma M), \\ &\text{If } \Sigma \text{ is odd: } (\Sigma M, \Sigma\bar{C}, \Sigma L). \end{aligned} \tag{20}$$

Note that the parity of these three words determines the signature $(+1,0,-1)$, which coincides with the signs of the first derivatives and signals a period-doubling bifurcation at the right end of the window. The actual width of a window, i.e., the stability range, is determined by the mapping function. Symbolic dynamics alone cannot say anything about it. In particular, a period-doubling sequence may shrink into a single point, as it is the case with piecewise linear maps with the slopes greater than one.

In general, symbolic description of a period-doubling sequence goes as follows. We write the preceding window as

$$(\lambda, \mu|_{\bar{C}}, \mu)$$

where λ and μ are symbolic sequences and $\mu|_{\bar{C}}$ denotes the sequence μ with its last letter replaced by $\bar{C}$, λ has even parity, whereas μ is odd. In addition, they differ only in the last letter, i.e., $\mu|_{\bar{C}} = \lambda|_{\bar{C}}$. The right (or upper) sequence μ goes into the next, period-doubled, lower sequence smoothly as $\mu\mu$ to ensure the correct even parity. The whole window then looks like

$$(\mu\mu, \mu\mu|_{\bar{C}}, \mu\lambda).$$

This process repeats *ad infinitum* to yield the entire period-doubling sequence. Beyond the accumulation point of the sequence there is a period-halving sequence of chaotic bands. The point where a period 2^n band merges into a period 2^{n-1} band is described by an infinite symbolic sequence formed from the upper and lower sequences of the corresponding period 2^n window as

$$\mu\lambda^{\infty}. \tag{21}$$

What has been said holds for general smooth one-dimensional mappings, including the unimodal and cubic maps.

Now consider a *symmetric* orbit described by a sequence $\Sigma C\bar{\Sigma}\bar{C}$. Let us disturb the orbit slightly, giving up the superstability but keeping the symmetry. The letter C may change to R or M by continuity, and $\bar{C}$ goes to L or M as the mirror image. The three words thus obtained may be ordered according to the parity of Σ to form a window

$$\begin{aligned} &\Sigma \text{ even: } (\Sigma M\bar{\Sigma}M, \Sigma C\bar{\Sigma}\bar{C}, \Sigma R\bar{\Sigma}L), \\ &\Sigma \text{ odd: } (\Sigma R\bar{\Sigma}L, \Sigma C\bar{\Sigma}\bar{C}, \Sigma M\bar{\Sigma}M). \end{aligned} \tag{22}$$

In contrast to windows, capable of undergoing period-doubling, this window has the signature $(+1,0,+1)$ and may be called an inversion point window in

accordance with our terms in Secs. 2 and 3. It is easy to check that the inversion window is equivalent to its mirror image (up to cyclic shifts, inessential due to periodicity). Only such a window undergoes a symmetry-breaking bifurcation, giving rise to an asymmetric window of the same period that starts a period-doubling sequence. Again, the upper sequence of the window (22) goes smoothly into the next window as the lower sequence of the latter. The upper sequence of the new window may be obtained by replacing the last letter to fit the -1 parity and the central word — by changing the last letter to $\bar{C}$. However, by taking the mirror image we get another window, not equivalent to the original one. This is nothing but the other symmetry-broken window. If the three words in the original window are maximal sequences, then the words in the mirror image window are minimal since the starting point is now located in the valley of the mapping function.

We illustrate what has been said by a few examples.

Example 1. The simplest symmetric superstable word is $C\bar{C}$. It extends to the inversion point window

$$(MM, C\bar{C}, RL). \tag{23}$$

This is the most clearly seen period 2 in the bifurcation diagram Fig. 2. By continuing RL to the lower sequence of the next window, we construct one of the asymmetric period 2 orbits as

$$(RL, R\bar{C}, RM). \tag{24}$$

Its mirror image, in terms of minimal sequences in descending order, is

$$(LR, LC, LM). \tag{25}$$

By cyclic shifting, the window (25) may be brought to maximal sequences

$$(RL, CL, ML). \tag{26}$$

Example 2. There is only one period 4 superstable orbit $RCL\bar{C}$. We write the whole bifurcation structure as:

$$(RMLM, RCL\bar{C}, RRLL)\begin{cases}(RRLL, RRL\bar{C}, RRLM)\\(RRLL, RCLL, RMLL).\end{cases} \tag{27}$$

Example 3. There are two symmetric orbits among the 30 period 6 windows[26,27] that allow symmetry-breaking bifurcation: $RMCLM\bar{C}$ and $RRCLL\bar{C}$. Among the 205 period 8 windows, only 5 can undergo symmetry breaking, namely:

$$RM^2CLM^2\bar{C}, RMLCLMR\bar{C}, R^2LCL^2R\bar{C},$$
$$R^2MCL^2M\bar{C}, R^3CL^3\bar{C}.$$

Therefore, we see that although symmetry breakings are always associated with orbits of even periods, only a few even periods are capable of doing so. Symbolic dynamics provides the selection rule.

If the inverse branches of the mapping are known explicitly, we can locate the symmetric and asymmetric superstable orbits exactly by the technique of "lifting" the corresponding symbolic sequence to an equation for the parameter value.[19,20] We return to the antisymmetric cubic map (1). Its inverse branches have been given in Eqs. (8). The sequence $\Sigma C\bar{\Sigma}\bar{C}$ describing a symmetric superstable orbit yields an equation

$$a = \Sigma(a, 0.5), \tag{28}$$

where we have used the definition (7) for a and the rescaling of the variables by $2C$. Take, for example, the period 6 orbit $RMCLM\bar{C}$, the final iteration equation reads

$$a_{n+1} = \cos\left(\frac{1}{3}\arccos\left(\frac{1}{a_n}\cos\left(\frac{1}{3}\arccos\left(\frac{0.5}{a_n}\right)-\frac{2\pi}{3}\right)\right)\right),$$

and leads to $A = 3a+1 = 3.46328\ldots$

An asymmetric superstable orbit $\bar{C}W\bar{C}\ldots$ yields the equation

$$a = W(a, -0.5). \tag{29}$$

The fact that the mirror image orbit $C\bar{W}C\ldots$ has the same parameter is a simple consequence of the symmetry property (9).

5. Symbolic Dynamics and Symmetry Restoration

We have mentioned in the Introduction that symmetry restoration has not been analyzed in the literature to date. In fact, symbolic dynamics provides us with a straightforward tool to accomplish this task. We recall[20] that the starting point of a periodic window

$$(\lambda, \mu|_{\bar{c}}, \mu)$$

which permits period-doubling, i.e., a window with $(+1, 0, -1)$ signature, corresponds to a band-merging point described by the sequence $\mu\lambda^\infty$. Applied to the period 2 symmetry-broken window (24), we locate the ending of the

symmetry-broken regime at

$$RM(RL)^{\infty}. \tag{30}$$

The very form of (30) tells the nature of this point. It corresponds to the "crisis" created by the collision of the unstable symmetric period 2 orbit, represented by $(RL)^{\infty}$, with the asymmetric chaotic attractor.

Its parameter value can be calculated from the following pair of "lifted" equations

$$\begin{aligned} a &= R \circ M(a,b), \\ a &= R \circ L(a,b), \end{aligned} \tag{31}$$

where the functions R, M, and L have been defined in Eqs. (8). The iterative solution of Eqs. (31) yields

$$A = 3.360893769096575 \ldots . \tag{32}$$

On the other hand, the mirror image of the window (24), i.e., window (26), corresponds to an asymmetric chaotic band, ending at

$$ML(RL)^{\infty}. \tag{33}$$

Referring to Eqs. (9), it is easy to verify that the parameter value of (33) is the same as that given by Eq. (32).

The symbolic sequence, corresponding to the symmetry restoration point, should have, so to speak, a "double personality". Seen from the left, it is asymmetric; seen from the right, it ought to be symmetric. Indeed, the sequences (30) and (33) are manifestly mirror images of each other, a property of symmetry-broken pairs. On the other hand, the symmetry has actually been restored since both sequences appear to be the $m \to \infty$ limit of the following periodic orbits, all located beyond the symmetry-restoration point (32):

$$RM(RL)^{m+1}ML(RL)^{m} = RM(RL)^{m}RLM(LR)^{m}L.$$

These orbits are nothing but the lower sequences of the inversion point window, formed by the symmetric periodic orbits

$$RM(RL)^{m}CLM(LR)^{m}\bar{C}, \tag{34}$$

which are equivalent to the cyclically shifted sequences

$$LM(LR)^m\bar{C}RM(RL)^mC, \tag{35}$$

as long as m remains finite. However, the $m\to\infty$ limits of (34) and (35) approach the asymmetric sequences (30) and (33), respectively.

It is interesting to investigate the rate of convergence of these periods towards the symmetry-restoration point, which may be considered as the $m=\infty$ member of the family (34). The corresponding superstable parameters may be determined by the word-lifting technique described in Sec. 4 and are listed in Table 1 (in the actual calculation we have kept more digits). The numbers δ_m are calculated from the formula

$$\delta_m=\frac{A_{m-2}-A_{m-1}}{A_{m-1}-A_m}.$$

These A_m's are asymptotically proportional to the length of the periods and converge much faster than the Feigenbaum period-doubling sequence, with the convergence rate $\delta=2.96455\ldots$, which coincides with the derivative

Table 1. Convergence towards the symmetry-restoration point.

m	Period	A_m	δ_m
0	6	3.41592 61947	
1	10	3.39439 31930	
2	14	3.37305 84369	
3	18	3.36519 01399	2.71148
4	22	3.36237 69478	2.79693
5	26	3.36139 92781	2.87745
6	30	3.36106 50252	2.92494
7	34	3.36095 16371	2.94786
8	38	3.36091 33022	2.95784
9	42	3.36090 03597	2.96193
10	46	3.36089 59924	2.96355
11	50	3.36089 45191	2.96417
12	54	3.36089 40221	2.96441
13	58	3.36089 38544	2.96450
14	62	3.36089 37978	2.96453
15	66	3.36089 37788	2.96455
16	70	3.36089 37723	2.96455
17	74	3.36089 37702	2.96455
18	78	3.36089 37695	2.96455
19	82	3.36089 37692	2.96455
20	86	3.36089 37691	2.96455
21	90	3.36089 37691	2.96455
⋮	⋮	⋮	
∞	∞	3.36089 37690	

$$u = f^{(2)'},$$

taken at the unstable 2-cycle $z^* \equiv (RL)^\infty$ of the parameter A_∞. This observation can be explained as follows. From Eq. (34) we have

$$f^{(3)}(A_m, \bar{C}) = f^{(-2m)}(A_m, C) \equiv z_m. \tag{36}$$

Denote by ε_m the parameter difference $A_\infty - A_m$. For m large enough,

$$\begin{aligned} &|z_m - z^*| \sim \varepsilon_m, \\ &\frac{\partial}{\partial x} f^{(2)}(A_m, x)|_{z_m} \sim u + \gamma \varepsilon_m, \end{aligned} \tag{37}$$

where γ is a constant independent of m. Thus, one has asymptotically

$$(u + \gamma \varepsilon_m)^m \varepsilon_m \sim 1,$$

which implies $\varepsilon_m \sim u^{-m}$ or $\delta = u$.

Symmetry restoration for higher periods may be analyzed in a similar way. Suppose there is a symmetric orbit $\Sigma C \bar{\Sigma} \bar{C}$. The inversion point window may be represented as

$$(\bar{\mu}\mu, \Sigma C \bar{\Sigma} \bar{C}, \rho\lambda), \tag{38}$$

where ρ, λ and μ are symbolic strings made of R, L and M, each having the parity of the corresponding letter. They are related to Σ and $\bar{\Sigma}$ in the following way:

$$\begin{aligned} \rho &= \text{the even one of } (\Sigma R, \Sigma M), \\ \mu &= \text{the odd one of } (\bar{\Sigma} M, \bar{\Sigma} L), \\ \lambda &= \text{the even one of } (\bar{\Sigma} M, \bar{\Sigma} L). \end{aligned} \tag{39}$$

In fact, ρ and λ, as well as μ and $\bar{\mu}$, are mirror images, and, in general, $\bar{\mu}$ differs from μ. Then the pair of asymmetric orbits is given by

$$\begin{aligned} &(\rho\lambda, \rho \bar{\Sigma} \bar{C}, \rho\bar{\mu}), \\ &(\lambda\rho, \lambda \Sigma C, \lambda\mu). \end{aligned} \tag{40}$$

The symmetry restoration point is described by

$$\rho\bar{\mu}(\rho\lambda)^{\infty} \text{ or } \lambda\mu(\lambda\rho)^{\infty}. \tag{41}$$

They are the $m \to \infty$ limits of the sequence of symmetric orbits

$$\Sigma_m C \bar{\Sigma}_m \bar{C}, \tag{42}$$

where

$$\Sigma_m = \rho\bar{\mu}(\rho\lambda)^m \text{ and } \bar{\Sigma}_m = \lambda\mu(\lambda\rho)^m. \tag{43}$$

It is worth mentioning that Eqs. (38) to (43) may be obtained from the simplest case of symmetry breaking and restoration, namely, that associated with the sequence $C\bar{C}$ and described by Eqs. (23) to (25) as well as Eqs. (30) through (35), by making the following substitutions:

$$\begin{aligned} R &\to \rho. \\ L &\to \lambda. \\ M &\to \bar{\mu}, \\ C &\to \Sigma C, \\ \bar{C} &\to \bar{\Sigma}\bar{C}. \end{aligned} \tag{44}$$

For the cubic map (1) all the superstability and symmetry restoration parameters may be calculated by solving the "lifted" equations. We have collected a few results in Table 2.

6. Discussion

Now we are in a position to make a few remarks in connection with previous observations of symmetry breakings in dynamical systems with an antisymmetry.

1. Asymmetry as "a necessary preliminary"[6] or "precursor"[15,18] to period-doubling appears to be a direct consequence of ordering of symbolic sequences. Although for differential equations, the only case of an explicit association of

Table 2. Symmetry breaking and restoration parameters.

Period	Σ	Symmetric	Asymmetric	Restoration	δ
2		2.5	3.12132 03436	3.36089 37691	2.96455
6	*RM*	3.34531 55584	3.46328 34578	3.46851 19419	2.83903
4	*R*	3.83081 15142	3.83989 44876	3.84470 61353	2.84205
6	*RR*	3.98179 73948	3.98189 90306	3.98195 41883	2.82018

symbolic dynamics to symmetry breaking seems to be the Lorenz system,[13] this fact calls for further application of symbolic dynamics to differential equations.

2. The observation that there exist period-doubling sequences which are not of the Feigenbaum type[5,28] may be better understood in light of our symbolic dynamics analysis. The authors of Ref. 5 put together the inversion windows of periods 2, 4 and 8, but skipped the period-doubling sequences, i.e., the true Feigenbaum sequences, that followed each symmetry breaking.

Of course, it is possible to select ordered period 2^n sequences in some way, other than Feigenbaum's. In Ref. 28 the same authors carried out a symbolic description for the period 2^n sequence in an antisymmetric map. In our notation the sequence may be generated in the following way. Starting from a symmetric orbit $\Sigma_1 C \bar{\Sigma}_1 \bar{C}$, construct the period-doubled sequence $\Sigma_2 C \bar{\Sigma}_2 \bar{C}$ by taking

$$\Sigma_2 = (\Sigma_1 C)_+ \bar{\Sigma}_1$$

where $(\Sigma C)_+$ means keeping the even sequence after changing C to R and M. This is equivalent to the simple substitutions

$$C \to R \text{ and } \bar{C} \to C \text{ for even } \Sigma_1,$$

$$C \to M \text{ and } \bar{C} \to C \text{ for odd } \Sigma_1,$$

in any symmetric orbit and then append its mirror image to get a word of double length. The process then repeats *ad infinitum*. The simplest choice $\Sigma_1 = b$ (blank) leads to the sequence

$$C\bar{C}$$

$$RCL\bar{C}$$

$$RRLCLLR\bar{C}$$

$$RRLRLLRCLLRLRRL\bar{C}$$

$$\ldots$$

that has been studied in Ref. 28. Clearly, there are infinitely many ways to choose Σ_1, e.g., $\Sigma_1 = RM$ leads to a 3×2^n sequence. These sequences converge much faster than the Feigenbaum case.

3. The observation of repeated bifurcations from symmetric orbit to asymmetric pair in the Duffing's equation, denoted as $P_s \to P_a^{\pm}$ in Ref. 10 fits well into the symbolic dynamics scheme of Sec. 4. It is worthwhile to work out the absolute nomenclature of periodic windows and to find the explicit symbolic dynamics of the model. Most probably, symbolic dynamics of three letters would provide the skeleton of the global bifurcation structure, as it was the case with the Lorenz model.[13]

4. In Ref. 2, a class of codimension 2 antisymmetric mappings was studied. A "new type" of bifurcation caused by the presence of a second parameter was associated with the symmetry breakings seen in the bifurcation diagram, although it had nothing to do with the latter. Their numerically measured value $a_{r3} \approx 3.361$ for the "next reverse bifurcation" is just the symmetry restoration point corresponding to $RM(RL)^{\infty}$, the exact value being given in the first row of Table 2.

Furthermore, the last, but not the least point concerns the study of symmetry restoration in differential equations. Symmetry restoration is inevitably associated with chaotic dynamics, as it occurs only in chaotic bands when a symmetric unstable orbit collides with the attractor. The phenomenon is not only associated with the first bifurcation that occurs when the nonlinearity gets strong enough, but exists in plenty for higher periods and larger parameter values. One must use symbolic dynamics as a guideline to understand the global systematics of the periodic and chaotic solutions.

After our preprint ASITP-88-035 of this paper has been distributed, we received a preprint of Szabó and Tél[29] which treats the symmetry breaking problem without explicit use of symbolic dynamics. We thank Szabó and Tél for sending the report.

Appendix. Proof of the Proposition of Section 3

To avoid clumsiness of notations, we consider only F and $F^{(2)}$, they may be replaced by $F^{(k)}$ and $F^{(2k)}$ everywhere below. We divide the proof into a few steps.

Step 1. Construct an auxiliary function

$$h(A, x) = F(A, x) + x;$$

the inversion point of F becomes a zero of h:

$$h(A^*, x^*) = 0.$$

Calculate the derivative

$$\left.\frac{\partial h}{\partial x}\right|_{x^*} = 2 \neq 0 \quad \text{(Condition 2)}.$$

Therefore, according to the implicit function theorem, there exists a function $x = x(A)$ such that

$$h(A, x(A)) = 0$$

in the vicinity of (A^*, x^*). In other words, an inversion points exists both above

and below A^*, but the stability may disappear on crossing A^*. In order to check the stability, we calculate the first partial derivative close to (A^*, x^*):

$$\frac{\partial F}{\partial x}(A^*+\delta,x)|_{x(A^*+\delta)} = 1+\left(\frac{\partial^2 F}{\partial x \partial A}\bigg|_* - \frac{1}{2}\frac{\partial F}{\partial A}\bigg|_* \frac{\partial^2 F}{\partial x^2}\bigg|_*\right)\delta + \ldots$$
$$= 1+\frac{1}{2}\frac{\partial^2 F^{(2)}}{\partial x \partial A}\bigg|_* \delta + \ldots \tag{45}$$

Therefore, as long as Condition 4 holds, the inversion point (and the 2-cycle formed by iterating it) will be stable on one side and unstable on the other side of A^*, depending on the sign of the mixed derivative. So far we have not studied the stability of 2-cycles by directly inspecting $F^{(2)}$. For this purpose:

Step 2. Construct another auxiliary function

$$g(A,x) = F^{(2)}(A,x) - x.$$

It is easy to see that both first partial derivatives vanish:

$$\frac{\partial g}{\partial x}\bigg|_* = \frac{\partial g}{\partial A}\bigg|_* = 0$$

due to the antisymmetry condition. Therefore, $g = 0$ is not a suitable relation to apply the implicit function theorem. Before going to the next step, we calculate two higher derivatives for later use:

$$\frac{\partial^2 g}{\partial x^2}\bigg|_* = 0,$$

$$\frac{\partial^3 g}{\partial x^3}\bigg|_* = 2S(F,x)|_* < 0 \quad \text{(Condition 3)}.$$

Step 3. The failure in choosing g was caused by the fact that $F^{(2)}$ contains the "trivial", 2-cycle formed by the inversion point studied in Step 1. It is better to exclude it beforehand. Thus, instead of g, we define

$$k(A,x) = \frac{g(A,x)}{h(A,x)}.$$

To calculate $k(A^*,x^*)$ and the derivatives, one encounters many uncertainties of the 0/0 type, which can be resolved by repeated use of *L*'Hospital rule, taking into

account the derivatives of h and g, calculated so far. The final results are:

$$k(A^*, \pm x^*) = 0,$$

$$\left.\frac{\partial k}{\partial x}\right|_{\pm^*} = 0,$$

$$\left.\frac{\partial k}{\partial A}\right|_{\pm^*} = \pm\frac{1}{2}\left.\frac{\partial^2 F^{(2)}}{\partial x \partial A}\right|_{\pm^*} \neq 0, \quad \text{(Condition 4)},$$

$$\left.\frac{\partial^2 k}{\partial x^2}\right|_{\pm^*} = \frac{1}{3}S(F,x)|_{\pm^*} < 0.$$

Therefore, according to the implicit function theorem, there exists function $A = A_+(x)$ and $A = A_-(x)$ such that

$$k(A_\pm(x), x) = 0$$

in the vicinities of $(A^*, \pm x^*)$, respectively. One can differentiate the above equation twice to get

$$\left.\frac{dA}{dx}\right|_{\pm^*} = 0,$$

$$\left.\frac{d^2A}{dx^2}\right|_{\pm^*} = -\frac{2}{3}\frac{S(F,x)|_*}{\left.\dfrac{\partial^2 F^{(2)}}{\partial x \partial A}\right|_*} \neq 0. \tag{46}$$

Clearly, $A = A_\pm(x)$, viewed as a function of x, have either a minimum or a maximum in A, depending on the sign of the mixed derivative in Condition 4. In addition, the convexity of $A = A_\pm(x)$ agrees with the sign of the δ term in Eq. (45), as both were determined by the same mixed derivative. The four branches of $A_+(x)$ and $A_-(x)$ form a pair of 2-cycles. There remains to check the stability of these 2-cycles by expanding the derivative $\partial F^{(2)}/\partial x$ in the neighbourhood of $(A^*, \pm x_*)$. Owing to Eqs. (46) and

$$\left.\frac{\partial^2 F^{(2)}}{\partial x^2}\right|_{\pm_*} = 0 \qquad \text{(consequence of antisymmetry)},$$

$$\left.\frac{\partial^3 F^{(2)}}{\partial x^3}\right|_{\pm_*} = 2S(F,x)|\pm_*,$$

the δx term vanishes in the expansion and we have

$$\frac{\partial F^{(2)}}{\partial x} = 1 + \frac{2}{3} S(F,x)|_{\pm *} (\delta x)^2 + \ldots .$$

Therefore, both 2-cycles are stable. Which 2-cycle is observed for a given initial value depends on the basin and the question goes beyond the scope of the local analysis of bifurcation theory.

References

1. R. M. May, *Ann. N.Y. Acad. Sci.* **316** (1979) 517.
2. H. Skjolding, B. Branner-Jorgensen, P. L. Christiansen, and H. E. Jensen, *SIAM J. Appl. Math.* **43** (1983) 50.
3. J. Testa and G. A. Held, *Phys. Rev.* **A28** (1983) 3085.
4. L. N. DaCosta, E. Knobloch, and N. O. Weiss, *J. Fluid Mech.* **109** (1981) 25.
5. J. Coste and N. Peyraud, *Phys. Lett.* **84A** (1981) 17.
6. E. Knobloch and N. O. Weiss, *Phys. Lett.* **85A** (1981) 127.
7. S. Novak and R. G. Frehlich, *Phys. Rev.* **A26** (1982) 3660.
8. M. R. E. Proctor and N. O. Weiss, *Rep. Prog. Phys.* **5** (1982) 1317.
9. C. Sparrow, *The Lorenz Equations, Bifurcations, Chaos, and Strange Attractors*, (Springer-Verlag, 1982).
10. S. Sato, M. Sano, and Y. Sawada, *Phys. Rev.* **A28** (1983) 1654.
11. K. A. Wiesenfeld, E. Knobloch, R. P. Miraoky, and J. Clark, *Phys. Rev.* **A29** (1984) 2102.
12. K. Kumar, A. K. Agarwal, J. K. Bhattacharjee, and K. Banerjee, *Phys. Rev.* **A35** (1987) 2334.
13. M-Z. Ding, and B.-L. Hao, *Commun. Theor. Phys.* **9** (1988) 375.
14. D. R. Moore, J. Toomre, E. Knobloch, and N. O. Weiss, *Nature* **303** (1983) 663.
15. D. D'Humieres, M. R. Beasley, B. A. Huberman, and A. Libchaber, *Phys. Rev.* **A26** (1982) 3483.
16. P. Bryant and C. Jeffries, *Phys. Rev. Lett.* **53** (1984) 250.
17. E. N. Lorenz, *J. Atmo. Sci.* **20** (1963) 130.
18. J. S. Swift and K. A. Wiesenfeld, *Phys. Rev. Lett.* **52** (1984) 705.
19. W.-Z. Zeng, B.-L. Hao, G.-R. Wang, and S.-G. Chen, *Commun. Theor. Phys.* **3** (1984) 283.
20. B.-L. Hao and W.-M. Zheng, *Int. J. Mod. Phys.* **B3** (1989) 235.
21. J. Guckenheimer, *Inventiones Math.* **39** (1977) 165.
22. W-Z. Zeng, M-Z. Ding, and J-N. Li, *Chinese Phys. Lett.* **2** (1985) 293; *Commun. Theor. Phys.* **9** (1988) 141.
23. W.-M. Zheng, "Construction of median itineraries for the antisymmetric cubic map", preprint ASITP-88-034.
24. W.-M. Zheng, "Construction of median itineraries without using the antiharmonic", preprint ASITP-88-006.
25. W.-M. Zheng, *J. Phys. A*, to appear.
26. W.-Z. Zheng, *Chinese Phys. Lett.* **2** (1985) 429; *Commun. Theor. Phys.* **8** (1987) 273.
27. B.-L. Hao and W.-Z. Zheng, in *XV International Colloquium on Group Theoretical Methods in Physics*, ed. R. Gilmore, (World Scientific, 1987).
28. J. Coste and N. Peyraud, *Physica* **5D** (1982) 415.
29. K. G. Szabó and T. Tél, "On the symmetry breaking bifurcation of chaotic attractors", ITP Budapest Report No. 462, 1988.

This article has been cited by:

1. Bai-lin Hao, Jun-Xian Liu, Wei-mou Zheng. 1998. Symbolic dynamics analysis of the Lorenz equations. *Physical Review E* **57**:5, 5378-5396. [CrossRef]
2. Wei-Mou Zheng. 1997. Predicting orbits of the Lorenz equation from symbolic dynamics. *Physica D: Nonlinear Phenomena* **109**:1-2, 191-198. [CrossRef]
3. Hai-Ping Fang, Bai-Lin Hao. 1996. Symbolic dynamics of the Lorenz equations. *Chaos, Solitons & Fractals* **7**:2, 217-246. [CrossRef]
4. A. Okni#ski, R. Rynio, J. Peinke. 1995. Symmetry-breaking and fractal dependence on initial conditions in dynamical systems: One-dimensional noninvertible mappings. *Chaos, Solitons & Fractals* **5**:5, 783-796. [CrossRef]
5. Fa-geng Xie, Bai-lin Hao. 1994. Counting the number of periods in one-dimensional maps with multiple critical points. *Physica A: Statistical Mechanics and its Applications* **202**:1-2, 237-263. [CrossRef]
6. Bai-lin Hao. 1991. Symbolic dynamics and characterization of complexity. *Physica D: Nonlinear Phenomena* **51**:1-3, 161-176. [CrossRef]
7. Wei-Mou Zheng. 1991. Symbolic dynamics for the Lozi map. *Chaos, Solitons & Fractals* **1**:3, 243-248. [CrossRef]